EurJOC
European Journal of Organic Chemistry

Research Article
doi.org/10.1002/ejoc.202300240

Chemistry Europe
European Chemical Societies Publishing

www.eurjoc.org

Exploitation of Dimeric Cyclic Cysteine as Helix Inducer in Ultra-Short Peptides for Cu(II)-Catalyzed Asymmetric Michael Addition on Chalcones

Giorgio Facchetti,*[a] Jaime Gracia Vitoria,[b] Martina Moraschi,[a] Raffaella Bucci,[a] Anne Catherine Abel,[c] Stefano Pieraccini,[c] Sara Pellegrino,*[a] and Isabella Rimoldi[a]

Dedicated to Prof. Cesare Gennari on the occasion of his 70th birthday.

A dimeric cyclic cysteine analogue, i.e. (1*R*,1′*R*,2*R*,2′*R*)-2,2′-disulfanediylbis (aminocyclohexane-1-carboxylic acid), was used as a constrained unnatural amino acid and as a folding inducer in ultra-short Leu-Val-containing peptide. Our results showed that both free dimer amino acid **L1** and its peptide derivative **L2** are able to chelate Cu(II). The obtained complexes resulted to be catalytically active in Michael addition reaction of nitromethane on different types of chalcones. **L1-Cu(II)** was shown more reactive in terms of conversion, while, in neat conditions, **L2-Cu(II)** allows to obtain an interesting 60% e.e. on pyridine chalcone.

Introduction

Unnatural amino acids (UAA) have gained significant attention in different fields due to their unique properties and chemical variability. Indeed, by tailoring the functional groups on the side chains it is possible to widen the scope of their applications, from medicine to materials science and catalysis. As an example, the introduction of UAAs in a biologically active peptide is one guiding principle for enhancing bioactivity and metabolic stability.[1] On the other hand, a high versatility in functions could be gained by exploiting UAAs self-organization ability. In this context, constrained UAAs could decrease the available conformational space by limiting the degrees of freedom and the entropic cost in peptide folding.[2]

The use of metal binding conformationally constrained UAAs could represent a valuable tool in the development of metal-based catalysts with high selectivity. This approach takes inspiration from metallo-enzymes that are able to catalyze chemical reactions with exquisite selectivity. Within the active site, the metal is coordinated to a unique pattern of amino acids adopting a structurally defined conformation responsible of the efficient substrate recognition and of the catalytic activity. Inspired by nature, chemists have been trying to develop catalytic systems able to keep unaltered the impressive activity typical of enzymes but introducing new reactivity.[3]

Metallopeptides are particularly useful as they combine enzyme selectivity with transition metal reactivity.[4] Conversely, the use of ultra-short peptides containing UAAs could be a relatively straightforward approach to reduce the molecular peptide complexity while keeping specificity. Gilbertson provided a pioneering example of asymmetric catalysis based on the use of phosphine containing amino acids as ligands in the palladium asymmetric addition of malonate to cyclopentenyl acetate. In this case, a β-turn secondary structure was induced upon metal binding, proving also to be responsible for enantioselectivity. Another example is given by L-proline supramolecularly linked to cobalt ions in enantioselective aldol reactions.[5]

In this paper, we investigated cyclic cysteine analogues in the stabilization of peptide secondary structure and in Cu(II) asymmetric catalysis. In particular, we were interested in investigating the dimeric compound (1*R*,1′*R*,2*R*,2′*R*)-2,2′-disulfanediylbis (aminocyclohexane-1-carboxylic acid) **L1** (Figure 1).[6] The presence of two free amino groups could indeed allow metal coordination, while the disulfide bridge and the cyclic constraints could induce the creation of a chiral catalytic pocket around the metal center. Compound **L1** was then used for the synthesis of its derivative **L2** containing the Leu-Val dipeptide at both the C-*termini* (Figure 1). We envisaged that, being **L1** a Cα-tetrasubstituted UAA, it could induce secondary structures when inserted in an ultra-short peptide stabilizing thus the catalytic pocket.[7]

On the other hand, we selected Leu-Val dipeptide because of its propensity to adopt an extended conformation due to the repulsion occurring between the aliphatic side chains, but also

[a] Dr. G. Facchetti, M. Moraschi, Dr. R. Bucci, Prof. S. Pellegrino, Prof. I. Rimoldi
Dipartimento di Scienze Farmaceutiche sezione di Chimica Generale e Organica "A. Marchesini"
Università degli Studi di Milano
Via Golgi 19, 20133 Milano (Italy)
E-mail: giorgio.facchetti@unimi.it
sara.pellegrino@unimi.it
[b] Dr. J. G. Vitoria
Vlaamse Instelling voor Technologisch Onderzoek
Boeretang 200, 2400 Mol (Belgium)
[c] Dr. A. C. Abel, Prof. S. Pieraccini
Dipartimento di Chimica
Università degli Studi di Milano
Via Golgi 19, 20133 Milano (Italy)

Supporting information for this article is available on the WWW under https://doi.org/10.1002/ejoc.202300240

Research Article
doi.org/10.1002/ejoc.202300240

Chemistry Europe
European Chemical Societies Publishing

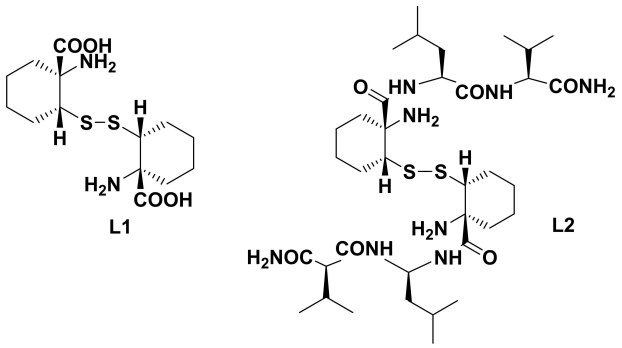

Figure 1. Structure of the constrained **L1** and **L2** cysteine derivatives.

because this sequence could fold in the presence of structuring amino acids.[8]

Conformational studies performed by NMR, CD and FTIR showed that **L2** indeed adopted a stable conformation, highlighting the structuring ability of the cysteine analogue. **L1** and **L2** were finally applied as chiral ligands in coordination to a Cu(II) center for the asymmetric Michael condensation reaction of nitromethane with a series of substituted chalcones. Both **L1** and **L2** ligands were found able to chelate Cu(II) and the obtained complexes are catalytically active.

Results and Discussion

The starting point for the synthesis of the constrained cysteine derivatives was the bicyclic sulfanyl thiazolidine **1**, produced through a Diels–Alder reaction and recently reported by the Cativiela research group.[6] The hydrolysis of the bicyclic compound **1** under microwave irradiation at 120 °C and the subsequent purification using DOWEX WX8 resin ion exchange chromatography led to product **3** and the desired dimer **L1**. (Scheme 1)

Indeed, the natural instability of **3** under the basic conditions (6% $NH_{3(aq)}$) used to elute the product during the purification was exploited to convert the mixture to the only

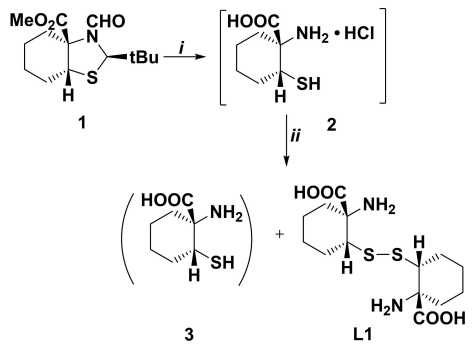

Reagents and conditions: ***i)*** **MW 120°C, 30 min;** ***ii)*** **Dowex® 50WX8, NH_3 aq. 6%**

Scheme 1. Synthesis of ligand **L1** from the bicyclic sulfanyl thiazolidine **1.**

oxidized **L1**, which could be recovered in high yield (95%). The synthesis of peptide **L2** was then undertaken according to the procedure described in Scheme 2. First, the protection of the free amine groups of **L1** was investigated. We tried to use tert-butoxy carbonyl anhydride in presence of *N*,*N*-diisopropylethylamine (DIPEA) in anhydrous CH_2Cl_2, according to the classical Boc protection methodology. However, this attempt was unsuccessful, thus we decided to try the reaction with a less steric hindered protecting group. Carboxybenzyl (Cbz) was selected and introduced using a protocol that temporarily protects the carboxylic acid moiety as trimethylsiloxy group by the slow addition of TMSCl over a solution of **L1** in anhydrous CH_2Cl_2 at 0 °C under stirring. 2.2 equivalents of Cbz-OSu were then added affording the protected compound **Cbz-L1** (85% yield) that was directly used for the following coupling reaction with H_2N-Leu-Val-$CONH_2$ dipeptide. The coupling reaction of **Cbz-L1** and the dipeptide H_2N-Leu-Val-$CONH_2$ was carried out in CH_2Cl_2 in presence of 1-ethyl-3-(3-dimethylaminopropyl) carbodiimide (EDC) and ethyl 2-cyano-2-(hydroxyimino)-acetate as activating agents and *N*,*N*-diisopropylethylamine (DIPEA) as base. The reaction led to the formation of dimeric peptide **4** in 89% yield after purification by recrystallization from CH_3OH/t-butyl methyl ether. Finally, compound **4** was deprotected in acetic acid with the addition of hydrobromic acid (33 wt.% in acetic acid) affording **L2** in quantitative yield (Scheme 2).

Compounds **4** and **L2** were fully characterized by NMR (for ^1H ^{13}C, COSY, TOCSY, HMBC, HMQC, NOESY experiments at 300 MHz, **4**: 9.6 mM solution in $CDCl_3$, **L2**: 10 mM solution in CD_3OH, see Supporting Information, Figures S2–S4 and Figures S5–S9). For compound **4**, a single set of signals corresponding to the monomer was observed in the ^1H NMR spectrum, indicating an equal spatial arrangement of the two parts of the dimeric peptide. The amide proton signals were also well dispersed, confirming the presence of a stable conformation as evinced also by the $J_{NH–CH\alpha}$ value of 8.8 Hz for NH-Val and of 5.2 Hz for NH-Leu. In variable temperature experiments, NH-Val showed a $\Delta\delta/\Delta T$ coefficient of 3.3 ppb/K, while NH-Leu of 1.5 ppb/K, highlighting their involvement in the formation of hydrogen bonds. On the other hand, NH-Cbz and $CONH_2$, showed $\Delta\delta/\Delta T$ coefficients higher than 5 ppb/K. NOESY experiments were then performed. A complete set of NH–NH n.o.e. signals was observed (Figure 2), indicating that a stable pseudo-helical conformation could be assumed by compound **4** in solution.

Compound **4** was then analyzed by CD and FTIR experiments to confirm NMR data. We observed in the CD spectrum a positive Cotton effect at around 190 nm and two negative minima at around 208 nm and 215 nm that confirmed the helix-like arrangement observed in the NMR. The deconvoluted FTIR spectrum of the amide-I region showed a single peak at 1657 cm^{-1} typical of helix structures, confirming the spectroscopic data as well (Figure 3).

In the case of *N*-free **L2** peptide, a different conformational behavior was observed. A single set of signals was detected in the ^1H NMR spectrum, but a downfield shift of NH values was highlighted. Furthermore, the $J_{NH–CH\alpha}$ value were of 8.7 Hz for NH-Val and of 8.1 Hz for NH-Leu, suggesting an extended

Research Article
doi.org/10.1002/ejoc.202300240

Chemistry Europe
European Chemical Societies Publishing

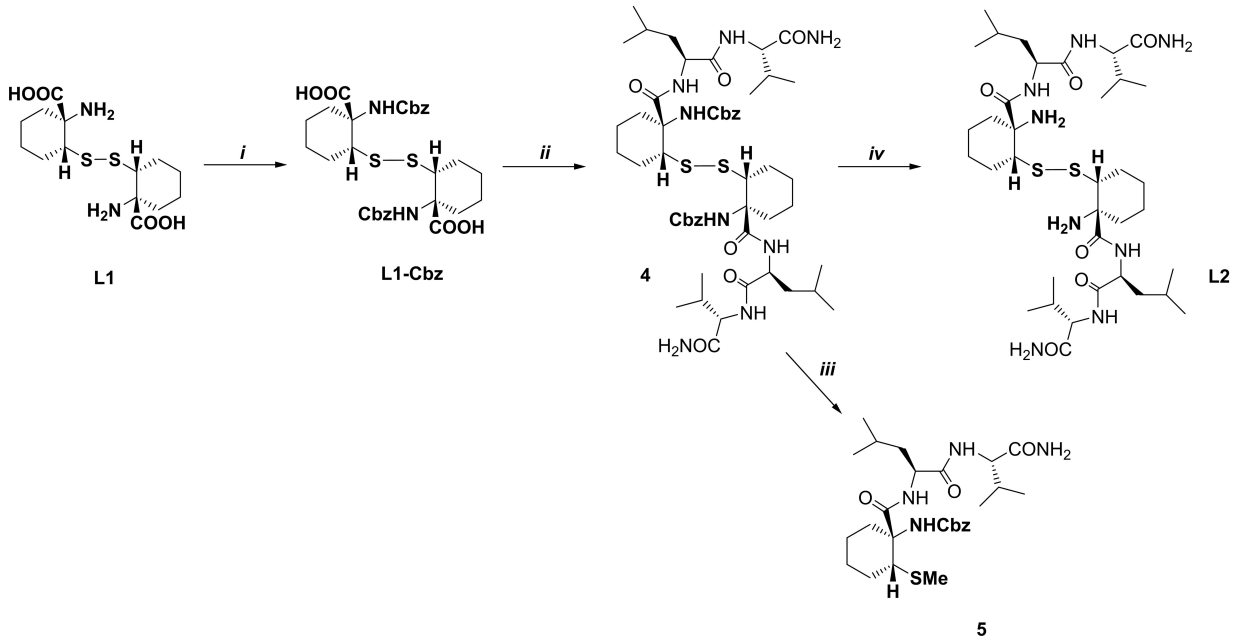

Reagents and conditions: ***i)*** **DIPEA (8 equiv.), TMSCl (6 equiv.), Cbz-OSu (2.2 equiv.), CH_2Cl_2, 0°C;** ***ii)*** **EtCN-oxime (3 equiv.), EDC (3 equiv.), CH_2Cl_2, 0°C, 1h; TFA-NH-Leu-Val-$CONH_2$ (3 equiv.), DIPEA (8 equiv.), rt, 1day;** ***iii)*** **nBu_3P (1.1 equiv.), THF, H_2O; CH_3I, TEA, THF, H_2O;** ***iv)*** **CH_3COOH, HBr (33 wt.% in acetic acid)**

Scheme 2. Synthetic pathway for the synthesis of the different constrained cysteine derivatives.

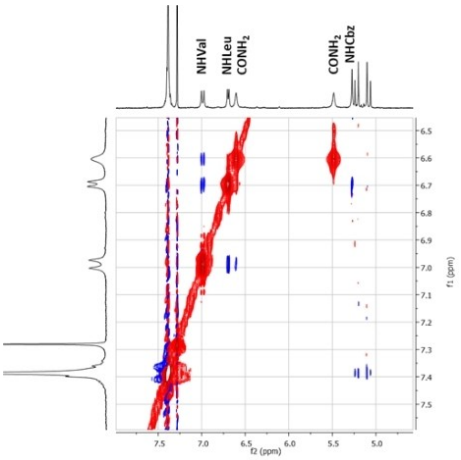

Figure 2. Expansion of –NH region in the NOESY spectrum of **4**.

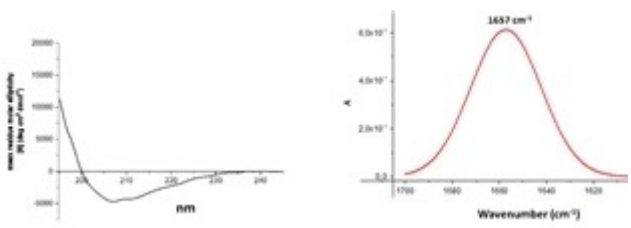

Figure 3. CD (on the left) and deconvoluted FTIR (on the right) spectra of compound **4** recorded in MeOH (100 μM).

conformation of the Leu-Val dipeptide. This is further indicated by the absence of NH–NH n.o.e. proximities, while NH–Hα and NH–Hβ Overhauser effects among vicinal amino acids were present. In variable temperature experiments, all the amide protons showed high $\Delta\delta/\Delta T$ coefficients, suggesting that they aren't involved in hydrogen bonds. CD experiments confirmed the different conformational tendency of **L2** peptide. **L2** CD signature is characterized by a strong negative band at around 200 nm and a slightly positive shoulder at around 220 nm (Figure 4 on the left), suggesting an extended conformation of the peptide.[9] In the FTIR deconvoluted spectrum (Figure 4 on the right), two peaks at 1611 cm^{-1} and 1661 cm^{-1} indicating that extended and turn-like conformation were present.[10]

In order to elucidate the different behavior of the protected and deprotected compounds, restrained Molecular Dynamics (rMD) simulations were performed[11] both in methanol and in

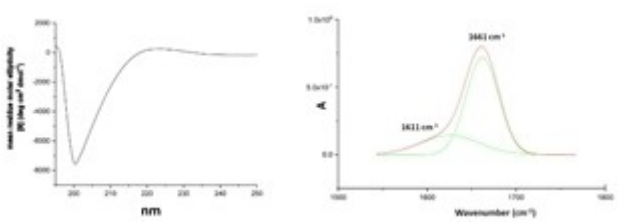

Figure 4. CD (on the left) and deconvoluted FTIR (on the right) spectra of compound **L2** recorded in MeOH (100 μM).

Research Article
doi.org/10.1002/ejoc.202300240

chloroform as solvents. The experimental distance restraints derived from NMR data for **L2** and **4** (See Supporting Information, Figure S10 and Table T1) have been enforced in simulations using a piecewise linear-harmonic restraint potential. rMD trajectories were submitted to cluster analysis to identify the prevailing structures in solution. Both in **L2** and **4**, more than 70% of the sampled structures belong to the three most populated clusters (Information about distribution within the clusters as well as structures are shown in Supporting Information, Table T2, Figures S11–13).

This suggests that both peptides tend to adopt a limited, well-defined set of conformations during the simulation. The central elements of the most populated clusters are reported in Figure 5. Interestingly, while **4** exhibits a helix-like shaped elongated structure promoted by hydrogen bonds (HBs) established by the oxygen of the benzoyl protecting group toward amide nitrogen of the peptide backbone, **L2** preferentially adopts a more compact, U-shaped conformation. In methanol, no persistent HB between the peptide strands at the two sides of the **L2** residue is observed as **L2** conformation keeps them 7–8 Å apart on average. This mirrors the NMR data showing no contact between the two strands as well as CD data. In $CHCl_3$ the structure as expected is more compact and some intramolecular HBs are detected during the simulation. Anyway, NMR spectra could not be recorded in chloroform due to insolubility of the compound. On the whole, rMD simulation accounts for the different behavior exhibited by **L2** and **4** in NMR and CD experiments and suggests the relevance of N-terminal protecting group in driving the conformational equilibrium of the peptides considered here.

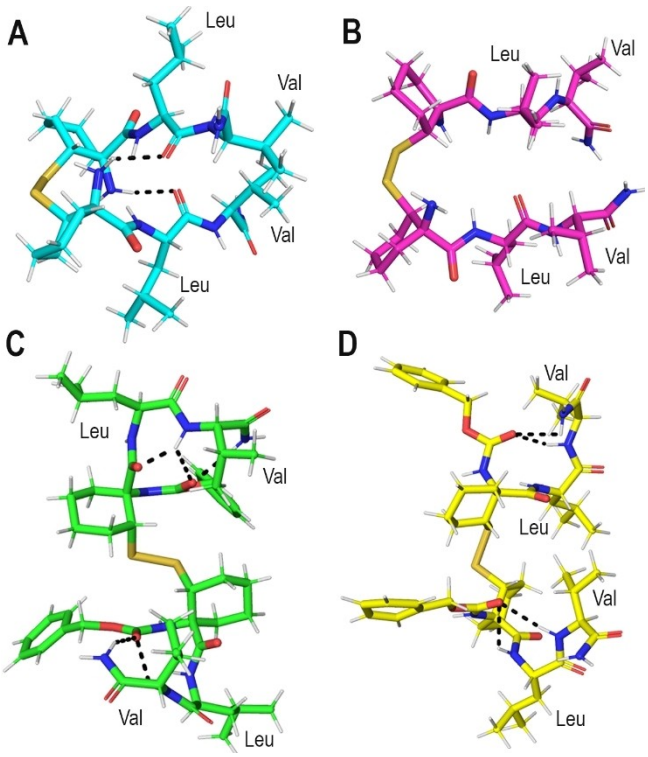

Figure 5. Structures of the most populated clusters for simulation of **L2** in chloroform (A) and methanol (B) and **4** in chloroform (C) and methanol (D). Structures are shown in stick representation, oxygen, nitrogen and sulfur atoms are colored in red, blue and dark yellow, respectively.

Finally, the monomeric tripeptide **5** containing a methyl tioether moiety hampering the sulfur oxidation to disulfide was synthesized starting from **4** (Scheme 2). A reduction reaction was conducted using *n*-tributylphosphine (1.1 equiv.) in THF.[12] Under this condition the desulfurization reaction occurred anyway, probably triggered by the phosphine reagent. In order to avoid this side reaction, a small aliquot of water (10% *v/v*) was added to the reaction mixture allowing to obtain monomeric version of **4** derivative that unfortunately was not stable, avoiding its isolation and characterization. A one pot reaction was thus developed in order to prevent the oxidation of the thiol group during purification processes. Compound **4** was dissolved in THF (4 mL for 0.12 g), then H_2O (40 equiv.) and *n*-Bu_3P were added to reduce the disulfide bond formation. After 5 min, TEA (pH > 8) and CH_3I (5 equiv.) were added to methylate the thiol group. The reaction was carried over 36 h and the purification by chromatography column afforded the desired product **5** in 60% yield. Compound **5** was characterized by NMR experiments at 300 MHz in $CDCl_3$ showing a good dispersion of the amide protons. Even for this compound a complete set of NH–NH n.o.e. signals were observed in NOESY experiments (see Supporting Information, Figure S16), while NH-Val showed a $\Delta\delta/\Delta T$ coefficient of 3 ppb/K, and NH-Leu of 1 ppb/K. On the other hand, CD analyses showed the presence of different conformations as suggested by a negative shoulder at around 208 nm. In the FTIR deconvoluted spectrum, the presence of both extended (1641 cm^{-1} peak) and turn (1663 cm^{-1}) ones (Figure 6) was confirmed. Taken together all the presented data highlighted that the cyclic cysteine derivative**2** is able to induce secondary structures when inserted in model peptides, but that this effect is higher when two unnatural moieties are presented in the sequence as in dimers **4** and **L2**.

Being assessed the conformational ability of the dimeric cyclic cysteine derivative in creating conformationally stable architectures, we then envisaged to apply **L1** and **L2** as chiral ligands in coordination to a Cu(II) center. Copper-based complexes have indeed gained an increasing attention for their earth-abundance and lower toxicity if compared to other transition metals. Moreover, the lower redox potentials of the different oxidation states available for copper, make its corresponding complexes more reactive towards organic cata-

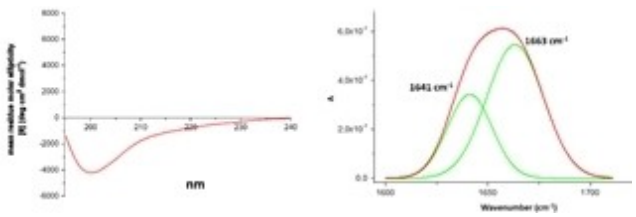

Figure 6. CD (on the left) and deconvoluted FTIR (on the right) spectra of **5** recorded in MeOH (100 μM).

Research Article
doi.org/10.1002/ejoc.202300240

lyzed transformations and able to undergo oxidative addition/reductive elimination reactions in a faster way. Here, we decided to explore **L1** and **L2** as ligands in the asymmetric Michael condensation reaction of nitromethane with a series of substituted chalcones. Michael addition using nitromethane represents a convenient way toward nitroalkanes, whose functionality can be easily converted into amine, ketone or carboxylic acid, providing a large series of interesting compounds. Asymmetric versions of this reaction were achieved thanks to chiral phase transfer catalysis, using either quaternary ammonium salts derived from the Cinchona alkaloids or organocatalysis using proline derivatives, thus leaving the enantioselective challenge in this reaction still to face to.[13] On the other hand, chalcone is the flavonoid core of many biologically relevant compounds derived from natural sources and thus considered as a privileged template in medicinal chemistry for drug discovery.[14]

The ability of copper to form a stable complex with both **L1** and **L2** was proved by UV-vis analysis (see Supporting Information, S18 and S19) and ESI-MS (see Supporting Information, S20 and S21). The complexes were simply synthesized by reacting copper acetate and the ligand (**L1** or **L2**) in toluene at room temperature. The formation of the complexes occurred immediately as confirmed by a change in the solution color from turquoise to light grey. This reaction commonly suffers from certain limitations, such as low reaction temperatures, high catalyst loading and use of strong acids as additives that make them still worth to be investigated.[15]

L1 was employed as chiral ligand in the presence of $Cu(OAc)_2 \cdot H_2O$ as metal precursor. The reaction was first performed on substrate **6a**, in toluene at rt (Table 1). Flame-dried CsF was used as the base as suggested by a procedure reported in literature for a similar application.[16] Indeed, the reaction is not working in the absence of CsF (Table 1, entry 5), while proceeds only when the copper salt (10% mol) and the ligand **L1** (11% mol) are both present. (Table 1, entries 1–4).

Then different reaction conditions were tested for **L1-Cu(II)** catalytic system, changing the solvent, substrate/catalyst ratio, basic additive and temperature (see Supporting Information, Table T3). Toluene was confirmed as the solvent of choice and CsF as the best performing base. With optimized conditions in hands, we expanded the reaction scope to differently substituted chalcones **6a–l** and **7** for the synthesis of the corresponding γ-nitro ketones (Table 2), versatile intermediates useful in the synthesis of biologically active γ-aminobutyric acids with potential GABAergic pathway modulation activity.[17]

A substrate/catalyst ratio of 10/1 was used for reaching a modest to quantitative conversion in 18 h at room temperature. In general, **L1** proved a more versatile ligand than **L2** affording the reaction products in moderate conversion accompanied with modest enantioselectivity with the highest e.e. obtained for the trifluoromethyl substituted substrate **6e** (34% e.e., Table 2, entry 8). A quantitative conversion with the catalytic system based on **L1** was achieved with chalcones carrying an electron withdrawing group on the benzoyl moiety (up to 99% for **6h**, **6i** and **6l**) but the reaction proceeded in an enantioselective way only on **6i** and **6j** (33% e.e. and 28% e.e.,

Table 1. Optimization of the reaction conditions in the asymmetric Michael addition on substrate **6a**.

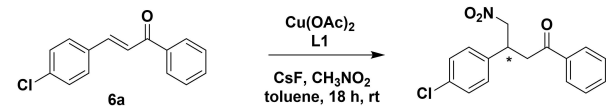

Entry	$Cu(OAc)_2 \cdot H_2O$	CsF [equiv.]	Ligand	Conversion [%][b]	e.e. [%][b]
1	10% mol	10	**L1**	66	7
2	10% mol	5	**L1**	66	29
3	10% mol	2.5	**L1**	37	25
4	10% mol	1	**L1**	24	*rac*
5	10% mol	–	**L1**	–	–
6	–	5	–	–	–
7	–	5	**L1**	–	–
8	10% mol	5	–	traces	–

Table 2. Asymmetric Michael addition on differently substituted chalcones.[a]

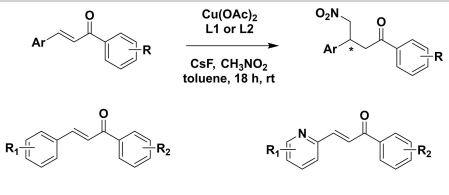

6a R_1 = *p*-Cl R_2 = H
6b R_1 = *m*-Cl; R_2 = H
6c R_1 = H; R_2 = H
6d R_1 = *m*-CF_3; R_2 = H
6e R_1 = *p*-CF_3; R_2 = H
6f R_1 = *m*-OMe ; R_2 = H
6g R_1 = *m*-NO_2 ; R_2 = H
6h R_1 = *p*-NO_2 ; R_2 = H
6i R_1 = H; R_2 = *m*-CF_3
6j R_1 = H; R_2 = *p*-CF_3
6k R_1 = H; R_2 = *m*-OMe
6l R_1 = H; R_2 = *m*-NO_2

7 R_1 = H; R_2 = H

Entry	substrate	Ligand	Conversion [%][b]	e.e. [%][b]
1	**6a**	**L1**	66	29
2	**6a**	**L2**	66	*rac*
3	**6b**	**L1**	57	*rac*
4	**6b**	**L2**	70	*rac*
5	**6c**	**L1**	59	17
6	**6d**	**L1**	84	21
7	**6d**	**L2**	85	*rac*
8	**6e**	**L1**	74	34
9	**6f**	**L1**	56	30
10	**6g**	**L1**	97	*rac*
11	**6g**	**L2**	73	*rac*
12	**6h**	**L1**	>99	*rac*
13	**6i**	**L1**	>99	33
14	**6j**	**L1**	62	28
15	**6j**	**L2**	45	*rac*
16	**6k**	**L1**	10	8
17	**6l**	**L1**	>99	*rac*
18	**7**	**L1**	>99	*rac*
19	**7**[c]	**L1**	15	16
20	**7**	**L2**	23	9
21	**7**[d]	**L2**	31	60

[a] Reaction conditions: CsF (5 equiv.), $Cu(OAc)_2 \cdot H_2O$ (10% mol, 0.8 mg), **L1** or **L2** (11% mol), substrate (1 mmol), CH_3NO_2 (10 equiv., 23 μL)), toluene (150 μL), 18 h, at room temperature [b] Conversions and enantiomeric excess (e.e.) were determined by chiral HPLC (see Supporting Information, Table T4, for the different conditions). If not indicated the first enantiomer is the predominant one. [c] Reactions were carried out in neat without the addition of base. [d] This reaction was carried out in neat in the presence of CsF (1 equiv.).

Research Article
doi.org/10.1002/ejoc.202300240

Table 2, entries 13–14 respectively). Conversely, catalyst **L2-Cu(II)** showed a marked lower reactivity as a general trend, although affording the product in satisfactory conversion for the R_1-substituted substrates. The reaction was then extended to the heterocycle chalcone **7** featuring a pyridine moiety, chosen in order to evaluate how the presence of an additional coordination site arising from the pyridinic nitrogen able to form potentially beneficial hydrogen bonding interactions with the catalyst, could modify the reactivity of these copper-based catalysts.[4c,18] Even in this case, **L1-Cu(II)** resulted more reactive than the **L2** analogue providing the product in quantitative conversion although any enantioselectivity was observed (table 2, entry 18). When **L2** was used as ligand, the conversion was dramatically decreased (Table 2, entry 20).

The reaction was then performed under solvent free conditions according to a recent paper reporting the detrimental effect of basic conditions on the enantioselectivity of the reaction involving the pyridine based chalcone.[19] Indeed, the reaction proceeded showing a certain level of enantioselectivity, i.e. 16% e.e. for **L1-Cu(II)** (Table 2, entry 19) whereas **L2-Cu(II)** afforded the product only in traces under totally free base conditions. Thus, with the aim to increase the conversion to an acceptable level, we decided to display the reaction with **L2-Cu(II)** under the same solvent free conditions but adding only one equivalent of CsF. Unexpectedly, not only an increase in the reaction conversion was achieved (from 23% to 31%) but also the enantioselectivity benefited from this variation and reaching a good 60% e.e. (Table 2, entry 21).

Conclusion

In conclusion, the unnatural cysteine derivative (1*R*,1′*R*,2*R*,2′*R*)-2,2′-disulfanediylbis (aminocyclohexane-1-carboxylic acid) **L1** was demonstrated as a powerful tool to stabilize secondary structure in Leu-Val containing peptide model **L2**. Furthermore, both **L1** and **L2** were found able to chelate Cu(II) with the obtainment of catalytic active complexes in asymmetric Michael reaction on differently substituted chalcones. Although the molecular complexity of ligand **L2** was found affecting the conversion rate of the reaction, a valuable 60% e.e. on pyridine chalcone **7** was obtained, under optimized reaction conditions in neat in the presence of 1 equiv. of CsF. Our results showed thus that the use of conformationally constrained amino acids could represent a powerful, although still less explored, tool toward the development of effective catalysts for asymmetric transformations.

Experimental Section

All reactions were carried out in oven-dried glassware and dry solvents under nitrogen atmosphere. MS analyses were performed with a Thermo Finnigan (MA, USA) LCQ Advantage system MS spectrometer with an electrospray ionization source and an 'Ion Trap' mass analyzer. The MS spectra were obtained by direct infusion of a sample solution in MeOH under ionization, ESI positive. Catalytic reactions were monitored by HPLC analysis with Merck-Hitachi L-7100 equipped with Detector UV6000LP and chiral column (AD Choralcelo, Lux Cellulose-4) ^{1}H NMR and ^{13}C NMR spectra were recorded with Varian Oxford 300 MHz spectrometer at 300 and 75 MHz, respectively. Chemical shifts are given as δ values in ppm relative to residual solvent peaks as the internal reference. ^{13}C NMR spectra are ^{1}H-decoupled, and the determination of the multiplicities was achieved by the APT pulse sequence.

Synthesis of (1*R*, 1′*R*, 2*R*, 2′*R*) −2,2′-disulfanediylbis (amino cyclohexane-1-carboxylic acid) L1: In a sealed tube bicyclic thiazolidine[6] **1** (3.07 mmol) was suspended in HCl 5 N (20 mL). The reaction was performed under microwave radiation for 3 h at 120 °C as far as the starting material had disappeared (TLC: n-hexane/AcOEt 7:3). Then, the aqueous layer was washed with diethylether (3×5 mL) and concentrated under vacuum. The obtained residue was purified by an ion exchange chromatography DOWEX WX8 resin. After purification, the solid was dissolved in aqueous NH_3 (6% v/v) and stirred overnight. Then, the solution was evaporated off furnishing **L1** as a white solid (1.02 g, 95% yield). m.p.: 215 °C (decomposes); ^{1}H NMR (D_2O, 400 MHz) δ ppm: 3.48 (dd, J = 12.7, 4.5, 2H), 2.23–2.13 (m, 2H), 2.02 (dd, J = 9.1, 3.4, 4H), 1.97–1.90 (m, 2H), 1.82–1.73 (m, 2H), 1.28–1.46 (m, 4H), 1.42–1.28 (m, 2H); ^{13}C NMR (D_2O, 100 MHz) δ ppm: 174.9, 64.6, 51.5, 33.8, 26.5, 24.9, 19.2; ESI-MS m/z calculated for $C_{14}H_{25}N_2O_4S_2$ 349.01; found 350.11 $[M+H]^+$; $[\alpha]_D^{23}$: +97 (c 0.9; H_2O).

Synthesis of (1*R*, 1′*R*, 2*R*, 2′*R*) −2,2′-disulfanediylbis ((((benzyloxy) carbonyl) amino) cyclohexane-1-carboxylic acid Cbz-L1: Over a solution of **L1** (200 mg, 0.57 mmol) in anhydrous CH_2Cl_2 (10 mL) at 0 °C, *N*,*N*-diisopropylethylamine (DIPEA) (0.8 mL, 4.59 mmol) and trimethylsilyl chloride (TMSCl) (0.44 mL, 3.45 mmol) were added. The mixture was allowed to stir for 30 min at 0 °C and *N*-(Benzyloxycarbonyloxy) succinimide (Cbz-OSu) (314.7 mg, 1.29 mmol) was added. After one day, the reaction was reloaded with Cbz-OSu (314.7 mg, 1.29 mmol). The reaction mixture was allowed to stir for 4 days at rt (TLC: hexane/AcOEt 3:7). Then, the solvent was evaporated off and the crude was partitioned between an aqueous solution of $NaHCO_3$ (5% w/w, 10 mL) and Et_2O (10 mL). The organic layer was discarded, and the aqueous layer was acidified with HCl 1 N until pH = 1. Then, the aqueous layer was extracted with AcOEt (3×10 mL) and the combined organic layers were washed with water (5 mL), dried under anhydrous Na_2SO_4, filtered off and concentrated under vacuum. The obtained white solid Cbz-L1 was subjected to the next reaction step without further purification (299.2 mg, 85% yield). m.p.: 185 °C (decomposes); ^{1}H NMR (300 MHz, CD_3OD) δ ppm: 7.52–7.18 (m, 5H), 5.16–4.99 (s, 2H), 4.97–4.78 (s, 2H), 3.68–3.48 (m, 1H), 2.68–2.53 (m, 2H), 2.46–2.08 (m, 2H), 2.00–1.79 (m, 2H), 1.72–1.35 (m, 2H); ^{13}C NMR (75 MHz, CD_3OD) δ ppm: 136.7, 133.9, 129.4, 128.8. 128.1, 128.0, 127.4, 127.3, 78.0, 66.0, 62.5, 53.9, 31.3, 27.1, 25.0, 24.8, 23.2, 20.8; ESI-MS m/z calculated for $C_{30}H_{36}N_2O_8S_2$ 616.82; found 617.91 $[M+H]^+$ $[\alpha]_D^{23}$: +60 (c 0.9; CH_3OH).

Synthesis of *N*-Boc-Leu-Val-CONH$_2$: Val-$CONH_2$ (1 g, 4.4 mmol) was dissolved in a mixture of CH_2Cl_2 (20 mL) and DMF (15 mL). The solution was cooled to 0 °C, then 1-ethyl-3-(3-dimethylaminopropyl) carbodiimide (EDC) (0.751 g, 4.84 mmol) and hydroxybenzotriazole (HOBt) (0.654 g, 4.84 mmol) were added. The reaction was allowed to stir at 0 °C for 1 h, then *N*-Boc-Leu (0.659 g, 4.4 mmol) and *N*,*N*-diisopropylethylamine (DIPEA) (1.53 mL, 8.8 mmol) were added (pH > 7). The reaction mixture was left under stirring overnight at rt. After this time, the solvent was evaporated under vacuum, then the crude residue was resuspended in CH_2Cl_2 (40 mL). The organic layer was washed with a 5% aqueous solution of $KHSO_4$ (10 mL), saturated solutions of $NaHCO_3$ (10 mL) and NaCl (10 mL). The resulting organic layer was dried over anhydrous Na_2SO_4, filtered off and concentrated under vacuum, affording *N*-Boc-Leu-Val-$CONH_2$ as a white solid (942.0 mg, 65% yield).

Synthesis of NH_2-Leu-Val-$CONH_2$: Compound *N*-Boc-Leu-Val-$CONH_2$ (0.25 g) was suspended in CH_2Cl_2 (10 mL), then the reaction was cooled to 0 °C and trifluoroacetic acid (TFA) (10 mL) was slowly added. The solution was allowed to stir at rt for 2 h. The solvent was evaporated under vacuum, affording NH_2-Leu-Val-$CONH_2$ as a white powder, in quantitative yield (174.0 mg). Characterization data are in accordance with those reported in literature.[20]

Synthesis of (1*R*, 1′*R*, 2*R*, 2′*R*) −2,2′-disulfanediylbis (amino-N-((S)-1-(((S)-1-amino-3-methyl-1-oxobutan-2-yl)amino)-4-methyl-1-oxopentan-2-yl) cyclohexane-1-carboxamide) 4: Over a solution of Cbz-L1 (100 mg, 0.16 mmol) in methylene chloride (5 mL) at 0 °C, EtCN-Oxime (69.2 mg, 0.49 mmol) and 1-ethyl-3-(3-dimethylaminopropyl) carbodiimide (EDC) (75.6 mg, 0.49 mmol) were added. The solution was stirred at 0 °C for 1 h and then NH_2-Leu-Val-$CONH_2$ (167.2 mg, 0.49 mmol) and *N*,*N*-diisopropylethylamine (DIPEA) (0.14 mL, 0.81 mmol) were added. The reaction mixture was stirring for 1 day at rt. After this time, the organic phase was washed with a saturated solution of $NaHCO_3$ (2 mL), a 5% aqueous solution of $KHSO_4$ (2 mL) and brine (2 mL). The resulting organic phase was dried over Na_2SO_4, filtered off and concentrated under vacuum. The residue was precipitated with CH_3OH/t-butyl methyl ether affording **4** as a white powder (148.0 mg, 89% yield). ^{1}H NMR (300 MHz, $CDCl_3$) δ ppm: 7.40–7.28 (m, 10H), 7.00 (d, J = 8.8 Hz, 2H), 6.70 (d, J = 5.2 Hz, 2H), 6.61 (s, 2H), 5.49 (s, 2H), 5.28–5.20 (m, 2H), 5.10–5.06 (m, 2H), 4.41–4.37 (dd, J = 8.7, 4.9 Hz, 2H), 4.23–4.18 (m, 2H), 3.67 (s, 2H), 3.34–3.32 (m, 2H), 2.59–2.45 (m, 3H), 2.10–2.08 (m, 2H), 1.79–1.60 (m, 9H), 1.48–1.44 (m, 4H), 1.30–1.28 (m, 6H), 1.00–0.89 (m, 24H); ^{13}C NMR (75 MHz, $CDCl_3$) δ ppm: 156.2, 136.5, 128.2, 128.1, 127.9, 127.7, 127.5, 68.9, 66.6, 63.2, 58.5, 54.2, 53.5, 49.4, 39.9, 31.1, 29.7, 27.3, 24.5, 24.4, 22.2, 20.6, 18.3, 16.9; ESI-MS m/z calculated for $C_{52}H_{78}N_8O_{10}S_2$: 1039.36, found 1062.04 $[M+Na]^+$

Synthesis of benzyl ((1R,2R)-1-(((S)-1-(((S)-1-amino-3-methyl-1-oxobutan-2-yl)amino)-4-methyl-1-oxopentan-2-yl)carbamoyl)-2-(methylthio)cyclohexyl)carbamate 5: Over a solution of the compound **4** (50 mg, 0.048 mmol, 1 equiv.) in THF (1 mL), water (100 μL) and subsequently $P(nBu)_3$ (13 μL, 0.053 mmol, 1.1 equiv.) were added and the reaction mixture was allowed to stir 5 min at rt. Then, triethylamine (TEA) (26.4 μL, 0.192 mmol, pH > 8) and CH_3I (14.9 μL, 0.24 mmol) were added to the solution. The reaction was stirred for 36 h at rt. The solvent was evaporated under vacuum and the crude residue was purified by silica gel chromatography using a gradient elution (from CH_2Cl_2 to AcOEt/CH_2Cl_2 9:1) affording compound **5** as a pale-yellow solid (16.0 mg, 60% yield). ^{1}H NMR (300 MHz, $CDCl_3$) δ ppm: 7.46–7.38 (m, 5H), 7.08 (d, J = 8.8 Hz, 1H), 6.70 (s, 1H), 6.58 (d, J = 4.5 Hz, 1H), 5.32–5.22 (m, 2H), 4.43 (dd, J = 8.8, 4.6 Hz, 1H), 4.24–4.20 (m, 1H), 3.02–3.00 (m, 1H), 2.59–2.49 (m, 2H), 2.08–2.02 (m, 3H), 1.98–1.93 (m, 1H), 1.77–1.61 (m, 6H), 1.45–1.27 (m, 5H), 1.01–0.88 (m, 12H); ^{13}C NMR (75 MHz, CDCl3) δ ppm: 173.5, 172.2, 155.4 135.7, 128.7, 128.2, 67.5, 64.0, 58.7, 54.2, 50.8, 40.3, 30.1, 29.6, 28.7, 25.6, 25.0, 23.2, 21.3, 20.0, 19.3, 16.9, 15.6; ESI-MS m/z calculated for $C_{27}H_{42}N_2O_5S$ 534.72; found 557.21 $[M+Na]^+$

Synthesis of (1*R*, 1′*R*, 2*R*, 2′*R*)-2,2′-disulfanediylbis(amino-N-((S)-1-(((S)-1-amino-3-methyl-1-oxobutan-2-yl)amino)-4-methyl-1-oxopentan-2-yl) cyclohexane-1-carboxamide) L2: 89.6 mg (1 equiv.) of compound 4 were dissolved in acetic acid (425 μL) and hydrobromic acid solution (33 wt.% in acetic acid, 425 μL). The solution was stirred at 40 °C for 30 min and evaporated under vacuum. The product **L2** was recrystallised from diethylether and 2-propanol affording a white solid (32.6 mg, 49% yield). ^{1}H NMR (300 MHz, CD_3OH) δ ppm: 8.84 (d, J = 8.7 Hz, 2H), 8.47 (m, 4H), 8.35 (d, J = 8.7 Hz, 2H), 7.42 (s, 2H), 7.01 (s, 2H), 4.11 (t, J = 4.7 Hz, 2H), 3.78–3.67 (m, 2H), 2.61–2.48 (m, 4H), 2.22–1.43 (m, 22 H), 1.04 (m, 12 H), 0.97 (m, 12 H); ^{13}C NMR (75 MHz, CD_3OH) δ ppm: 174.1, 173.9, 64.7, 59.8, 53.8, 52.0, 41.5, 35.3, 31.0, 30.1, 24.8, 24.7, 22.5, 19.9, 19.3, 18.3, 17.8; ESI-MS m/z calculated for $C_{36}H_{66}N_8O_6S_2$ 770.45, found 771.60 $[M+H]^+$, 793.69 $[M+Na]^+$

General procedure for the asymmetric Michael addition to chalcones 6a–l

A mixture of powdered, flame-dried CsF (5 equiv.), ligand **L1** or **L2** (11% mol), $Cu(OAc)_2 \cdot H_2O$ (10% mol., 0.8 mg), and chalcone (1 mmol) in toluene (150 μL) was treated with nitromethane (10 equiv. 23 μL). The mixture was stirred at rt for 18 h and then diluted with 400 μL of Et_2O and 400 μL of H_2O. The organic layer was separated, dried over Na_2SO_4 and evaporated. The conversion and the enantiomeric excess were determined by HPLC analysis.[4c]

General procedure for the asymmetric Michael addition to heterocycle chalcone 7

Chalcone containing pyridine 7 was synthesized as reported in literature.[21] In a capped vial containing $Cu(OAc)_2 \cdot H_2O$ (10% mol., 0.8 mg) and the ligand L1 or L2 (11% mol) were added the substrate (1 mmol) and nitromethane (20 equiv.) and the resulting mixture was stirred at room temperature for 18 h then diluted with 400 μL of Et_2O and 200 μL of H_2O. The organic layer was separated, dried over Na_2SO_4 and evaporated. The conversion and the enantiomeric excess were determined by HPLC analysis.

Computational methods

The initial conformations of L2 and 4 were generated in Moloc[22] by energy minimization in a MAB force field. Then non-natural aminoacid L2 has been parametrized according to standard procedures described in Supporting Information. rMD simulations were performed in explicit solvent (either $CHCl_3$ or methanol) using periodic boundary conditions. Both peptides were solvated in a cubic solvent box with 15 Å buffer. The ff14SB[23] forcefield was used for the amino acids and the GAFF force field,[24] developed for joint use with Amber FFs, has been used for the non-natural residues. The peptides were submitted to a 10000 steps geometry optimization using the steepest descent algorithm followed by a two-stage equilibration phase composed by 200 ps long NVT rMD followed by further 200 ps in the NPT ensemble. NMR restraints were enforced during the simulation with a piecewise linear-harmonic restraint potential. The exact form of the potential is described in MD Supporting Information Figure S10, as well as the exact distance restraints in MD Supporting Information Table T1.

Simulations were run on GPU-accelerated GROMACS 2016 for 1 μs, with a 2 fs time steps and in the NPT ensemble. Temperature was kept constant to the target value (300 K) with the v-rescale algorithm[25] while pressure was held constant (1 Bar) with the Berendsen algorithm.[26] Clustering of the obtained structures was done using the GROMOS algorithm[27] with a threshold of 2.0 Å in gmx cluster. For each simulation 10001 structures were extracted for analysis and the exact number of clusters, distribution of clusters and percentage of the total are given in Supporting Information Table T2 and Figure S11. Structures were visualized, the structures for the second and third most poluated clusters are shown in MD Supporting Information Figure S12 and S13, figures were generated with PyMol, The PyMOL Molecular Graphics System, Versio 2.3.4 Schrödinger, LLC.

Acknowledgements

The authors thank Dr. Iñaki Osante and Prof. Carlos Cativiela (University of Zaragoza) for providing compound 1 and Carlo Lapidari for pratctical help in the synthesis of compounds L1 and L2.

Conflict of Interests

The authors declare no conflict of interest.

Data Availability Statement

The data that support the findings of this study are available in the supplementary material of this article.

Keywords: cysteine · Cu(II) complex · helix · michael addition · unnatural amino acid

[1] a) J. Liu, J. Han, K. Izawa, T. Sato, S. White, N. A. Meanwell, V. A. Soloshonok, *Eur. J. Med. Chem.* **2020**, *208*, 112736; b) E. Lenci, A. Trabocchi, *Chem. Soc. Rev.* **2020**, *49*, 3262–3277; c) A. Contini, N. Ferri, R. Bucci, M. G. Lupo, E. Erba, M. L. Gelmi, S. Pellegrino, *Pept. Sci.* **2018**, *110*, e23089.

[2] a) W. S. Horne, T. N. Grossmann, *Nat. Chem.* **2020**, *12*, 331–337; b) R. Bucci, F. Foschi, C. Loro, E. Erba, M. L. Gelmi, S. Pellegrino, *Eur. J. Org. Chem.* **2021**, *2021*, 2887–2900.

[3] a) M. Wittwer, U. Markel, J. Schiffels, J. Okuda, D. F. Sauer, U. Schwaneberg, *Nature Catalysis* **2021**, *4*, 814–827; b) M. T. Reetz, *Acc. Chem. Res.* **2019**, *52*, 336–344; c) M. Pellizzoni, G. Facchetti, R. Gandolfi, M. Fusè, A. Contini, I. Rimoldi, *ChemCatChem* **2016**, *8*, 1665–1670; d) G. Facchetti, I. Rimoldi, *New J. Chem.* **2018**, *42*, 18773–18776; e) G. Facchetti, S. Pellegrino, R. Bucci, D. Nava, R. Gandolfi, M. S. Christodoulou, I. Rimoldi, *Molecules* **2019**, *24*, 2771; f) G. Facchetti, R. Bucci, M. Fusè, E. Erba, R. Gandolfi, S. Pellegrino, I. Rimoldi, *Inorg. Chem.* **2021**, *60*, 2976–2982; g) G. Facchetti, R. Bucci, M. Fusè, I. Rimoldi, *ChemistrySelect* **2018**, *3*, 8797–8800.

[4] a) A. J. Metrano, S. J. Miller, *Acc. Chem. Res.* **2019**, *52*, 199–215; b) S. Pellegrino, G. Facchetti, A. Contini, M. L. Gelmi, E. Erba, R. Gandolfi, I. Rimoldi, *RSC Adv.* **2016**, *6*, 71529–71533; c) I. Rimoldi, R. Bucci, L. Feni, L. Santagostini, G. Facchetti, S. Pellegrino, *J. Pept. Sci.* **2021**, *27*, e3289.

[5] a) S. R. Gilbertson, G. Chen, M. McLoughlin, *J. Am. Chem. Soc.* **1994**, *116*, 4481–4482; b) S. R. Gilbertson, S. E. Collibee, A. Agarkov, *J. Am. Chem. Soc.* **2000**, *122*, 6522–6523.

[6] J. Gracia-Vitoria, I. Osante, C. Cativiela, P. Merino, T. Tejero, *J. Org. Chem.* **2018**, *83*, 12471–12485.

[7] a) M. Crisma, C. Toniolo, *Pept. Sci.* **2015**, *104*, 46–64; b) A. Ruffoni, A. Contini, R. Soave, L. Lo Presti, I. Esposto, I. Maffucci, D. Nava, S. Pellegrino, M. L. Gelmi, F. Clerici, *RSC Adv.* **2015**, *5*, 32643–32656.

[8] a) F. Oliva, R. Bucci, L. Tamborini, S. Pieraccini, A. Pinto, S. Pellegrino, *Front. Chem.* **2019**, *7*, 133; b) R. Bucci, A. Contini, F. Clerici, S. Pellegrino, M. L. Gelmi, *Org. Chem. Front.* **2019**, *6*, 972–982.

[9] N. J. Greenfield, *Nature Protocols* **2006**, *1*, 2876–2890.

[10] A. Sadat, I. J. Joye, *Appl. Sci.* **2020**, *10*, 5918.

[11] F. Oliva, R. Bucci, L. Tamborini, S. Pieraccini, A. Pinto, S. Pellegrino, *Front. Chem.* **2019**, *7, 133*.

[12] J. A. Karas, N. A. Patil, J. Tailhades, M.-A. Sani, D. B. Scanlon, B. E. Forbes, J. Gardiner, F. Separovic, J. D. Wade, M. A. Hossain, *Angew. Chem. Int. Ed.* **2016**, *55*, 14743–14747; *Angew. Chem.* **2016**, *128*, 14963–14967.

[13] a) X. Huang, W. Zhang, *Chem. Commun.* **2021**, *57*, 10116–10124; b) H.-w. Wang, T. Oriyama, *Chem. Lett.* **2018**, *47*, 472–474; c) S. D. Pasuparthy, B. Maiti, *ChemistrySelect* **2022**, *7*, e202104261.

[14] C. Zhuang, W. Zhang, C. Sheng, W. Zhang, C. Xing, Z. Miao, *Chem. Rev.* **2017**, *117*, 7762–7810.

[15] a) M. Meazza, V. Polo, P. Merino, R. Rios, *Org. Chem. Front.* **2018**, *5*, 806–812; b) M. Lu, H. Li, C. Zou, J. Li, C. Liu, M. Sun, Y. Ma, R. Cheng, J. Ye, *Org. Biomol. Chem.* **2019**, *17*, 9305–9312; c) R. Kumar, M. K. Jaiswal, R. P. Singh, *Asian J. Org. Chem.* **2020**, *9*, 1576–1580.

[16] E. J. Corey, F.-Y. Zhang, *Org. Lett.* **2000**, *2*, 4257–4259.

[17] a) C. N. Kent, C. Park, C. W. Lindsley, *ACS Chem. Neurosci.* **2020**, *11*, 1740–1755; b) C. Guo, M. Saifuddin, T. Saravanan, M. Sharifi, G. J. Poelarends, *ACS Catal.* **2019**, *9*, 4369–4373; c) J. H. Shim, Y. Hong, J. H. Kim, H. S. Kim, D.-C. Ha, *Catalysts* **2021**, *11*, 1134; d) L. Biewenga, T. Saravanan, A. Kunzendorf, J.-Y. van der Meer, T. Pijning, P. G. Tepper, R. van Merkerk, S. J. Charnock, A.-M. W. H. Thunnissen, G. J. Poelarends, *ACS Catal.* **2019**, *9*, 1503–1513.

[18] G. Blay, C. Incerti, M. C. Muñoz, J. R. Pedro, *Eur. J. Org. Chem.* **2013**, *2013*, 1696–1705.

[19] G. Zhang, C. Zhu, D. Liu, J. Pan, J. Zhang, D. Hu, B. Song, *Tetrahedron* **2017**, *73*, 129–136.

[20] V. P. Romanova, V. V. Shilin, *Ukr. Khim. Zh. (Russ. Ed.)* **1989**, *55*, 527.

[21] G. Facchetti, M. Fusè, T. Pecoraro, D. Nava, I. Rimoldi, *New J. Chem.* **2021**, *45*, 18769–18775.

[22] P. R. Gerber, K. Muller, *J. Comput.-Aided Mol. Des.* **1995**, *9*, 251–268.

[23] J. A. Maier, C. Martinez, K. Kasavajhala, L. Wickstrom, K. E. Hauser, C. Simmerling, *J. Chem. Theory Comput.* **2015**, *11*, 3696–3713.

[24] J. Wang, R. M. Wolf, J. W. Caldwell, P. A. Kollman, D. A. Case, *J. Comput. Chem.* **2004**, *25*, 1157–1174.

[25] G. Bussi, D. Donadio, M. Parrinello, *J. Chem. Phys.* **2007**, *126*, 014101.

[26] H. J. C. Berendsen, J. P. M. Postma, W. F. V. Gunsteren, A. DiNola, J. R. Haak, *J. Chem. Phys.* **1984**, *81*, 3684–3690.

[27] X. Daura, K. Gademann, B. Jaun, D. Seebach, W. F. V. Gunsteren, A. E. Mark, *Angew. Chem. Int. Ed.* **1999**, *38*, 236–240; *Angew. Chem.* **1999**, *111*, 249–253.

Manuscript received: March 15, 2023
Revised manuscript received: April 5, 2023
Accepted manuscript online: April 13, 2023